Inorganic Chemistry Communications 161 (2024) 112016

Contents lists available at ScienceDirect

Inorganic Chemistry Communications

journal homepage: www.elsevier.com/locate/inoche

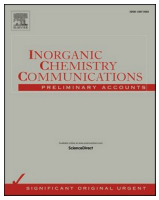

Short communication

Enriched adsorption of methyl orange by zinc doped lithium manganese oxides nanosorbent

Pooja R. Popat [a], Abeer Yousef Alyami [b], Gajendra Kumar Inwati [c], Bharat A. Makwana [d,*], Maha Awjan Alreshidi [e], Jari S. Algethami [b,f], Mohamed Abbas [g], Krishna Kumar Yadav [h,i,*]

[a] Department of Chemistry, HVHP Institute of Post Graduate Studies and Research, Kadi Sarva Vishwavidyalaya, Kadi, Gujarat, India
[b] Department of Chemistry, College of Science and Arts, Najran University, P.O. Box, 1988, Najran 11001, Saudi Arabia
[c] School of Chemical Sciences, Devi Ahilya Vishvidyalaya, Indore, Madhya Pradesh 452001, India
[d] Department of Chemistry, Bhavan's Sheth R.A. College of Science, Gujarat University, Ahmedabad, India
[e] Department of Chemistry, University of Hail, Saudi Arabia
[f] Advanced Materials and Nano-Research Centre (AMNRC), Najran University, Najran 11001, Saudi Arabia
[g] Electrical Engineering Department, College of Engineering, King Khalid University, Abha 61421, Saudi Arabia
[h] Faculty of Science and Technology, Madhyanchal Professional University, Ratibad, Bhopal 462044, India
[i] Environmental and Atmospheric Sciences Research Group, Scientific Research Center, Al-Ayen University, Thi-Qar, Nasiriyah 64001, Iraq

ARTICLE INFO

Keywords:
Adsorption
Nanosorbents
Metal oxides
Calcination
Langmuir and Freundlich isotherm
Methyl orange

ABSTRACT

In this work, zinc-doped lithium manganese oxide ($LiMn_2O_4$: Zn) nanosorbent was synthesized by simple calcination technique, and the protonated H/$LiMn_2O_4$: Zn was explored to resolve the environmental issues such as removing organic molecules from wastewater. The crystalline size of 26 nm of cubic HMn_2O_4: Zn (space group: Fd-3m) by the X-ray Diffraction while the TEM sizes were obtained 14.3 and 13 nm for $LiMn_2O_4$: Zn and HMn_2O_4: Zn. The chemical states of the structurally modified HMn_2O_4: Zn were determined by X-ray Photoelectron Spectroscopy. The surface area of 84.98 (m^2/g) along with a total pore volume of 0.2061 (cm^3/g) was examined by BET, respectively. The results demonstrated that Nanosorbent effectively adsorbs methyl orange in an acidic solution (pH = 3) during the course of 180 min of contact time. The adsorption efficiency of HMn_2O_4: Zn nanosorbents for methyl orange was evaluated by applying Langmuir and Freundlich isotherm. However, the HMn_2O_4: Zn nanosorbents showed efficient adsorption towards methyl orange dye which may be further applied to remove the different organic dye molecules from wastewater.

1. Introduction

Water is an absolute necessity in our daily lives therefore it is necessary to preserve water and prevent contamination of water via different pollutants. Water contamination has become a significant issue in recent years as a result of human activities. Sewage, industry, and agriculture have all been blamed for water contamination in the past. There is a severe water shortage, stressing the urgent need for year-round food production to combat hunger, poverty, and malnutrition, necessitating wastewater reuse for irrigation [1]. Therefore, effective wastewater treatment is required.

An Industrial discharge contains huge numbers of heavy metals and chemicals like Sulphur, asbestos, noxious solvents, polychlorinated biphenyls, lead, mercury, nitrates, phosphates, acids, alkali, dyes, pesticides, benzene, carbon tetrachloride, toluene, and volatile organic chemicals which are responsible for the contamination of water [2–4].

A dye is a colored material that binds to the substrate it is applied on chemically. Dyes are conjugated molecules that are made up of aromatic and/or unsaturated chemicals that are derived from natural sources or synthesized. Both synthetic and natural colors have their uses in day-to-day living. Dyes containing wastewater comprise a huge amount of toxic, carcinogenic, mutagenic, and teratogenic elements which can cause serious damage to biological organisms and many others due to their potential toxicity of dyes [5]. Water-soluble azo dye methyl orange is widely utilized in research labs as well as the textile, printing, paper, culinary, and pharmaceutical industries. Since the dye's aqueous solution has a pH of roughly 6.5, it can act as a weak acid, which is why it is mostly utilized as an acid-base indicator in analytical chemistry

* Corresponding authors at: Faculty of Science and Technology, Madhyanchal Professional University, Ratibad, Bhopal 462044, India (K.K.Y.). Bhavan's Sheth R.A. College of Chemistry, Gujarat University Ahmedabad, 380001 Gujarat, India (B.A.M).
E-mail addresses: bhrtchem1@gmail.com (B.A. Makwana), envirokrishna@gmail.com (K.K. Yadav).

https://doi.org/10.1016/j.inoche.2023.112016
Received 11 August 2023; Received in revised form 10 December 2023; Accepted 31 December 2023
Available online 6 January 2024

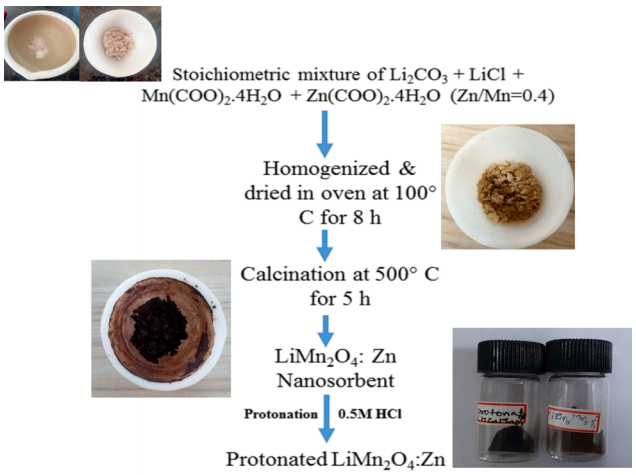

Fig. 1. Systematic representation for the synthesis of $LiMn_2O_4$: Zn nano sorbent.

laboratories. Aquatic life is poisoned by this dye. Acute exposure to this hazardous dye can result in tissue necrosis, an increase in heart rate, vomiting, shock, cyanosis, and jaundice in humans. Although the dye's toxicity has not yet been fully measured, its high concentration in biological systems may be detrimental[6]. Hence, before the wastewater generated by different industries is released into the environment, it is crucial to remove this dye from it [7,8].

There are several methods for wastewater treatment which can be mainly classified as physical, chemical, and biological. The physical method includes coagulation, membrane separation, adsorption, filtration, flotation, etc. The chemical method includes oxidation, reduction, and electrochemical methods. While the biological method includes aerobic and anaerobic degradation [9]. Previously coagulation process for dye removal was performed by Lau et al. [10]. Wensong et al. prepared a biomimetic dynamic membrane for the removal of aquatic dye [11]. Chemical oxidation method for methylene blue removal done by Dutta et al. [12]. Noxious pollutant removal made by TiO_2 nanoparticles with activated carbon [13]. Among all these physical adsorption is one of the best method for wastewater treatment due to its low cost and good efficiency [14].

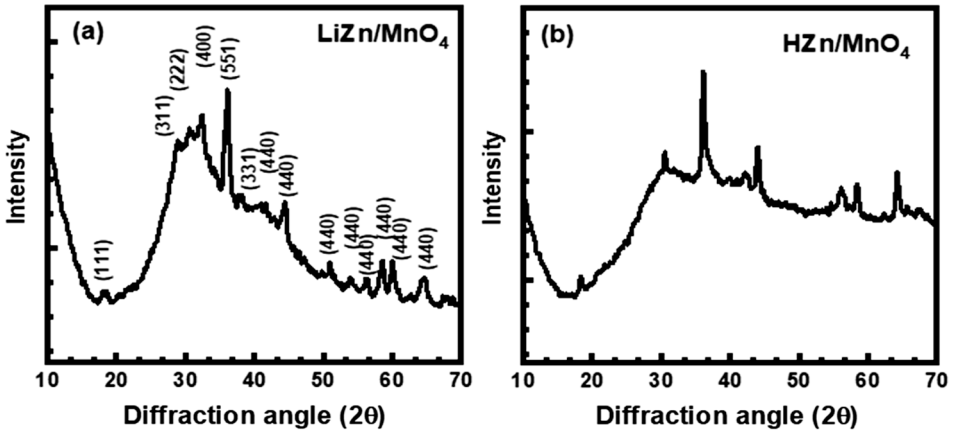

Fig. 2. X-ray Diffraction pattern of $LiMn_2O_4$: Zn and HMn_2O_4: Zn.

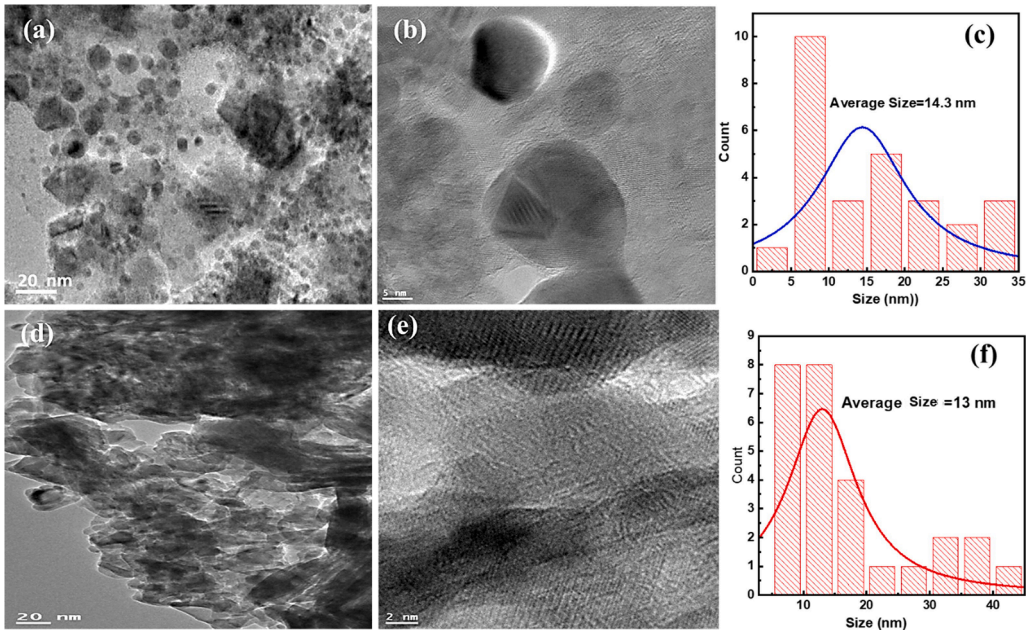

Fig. 3. HRTEM analysis: (a) Monograph of $LiMn_2O_4$: Zn (b) HR image of $LiMn_2O_4$: Zn (c) Histogram of $LiMn_2O_4$: Zn (d) Monograph of HMn_2O_4: Zn (e) HR image of HMn_2O_4: Zn (f) Histogram of HMn_2O_4: Zn.

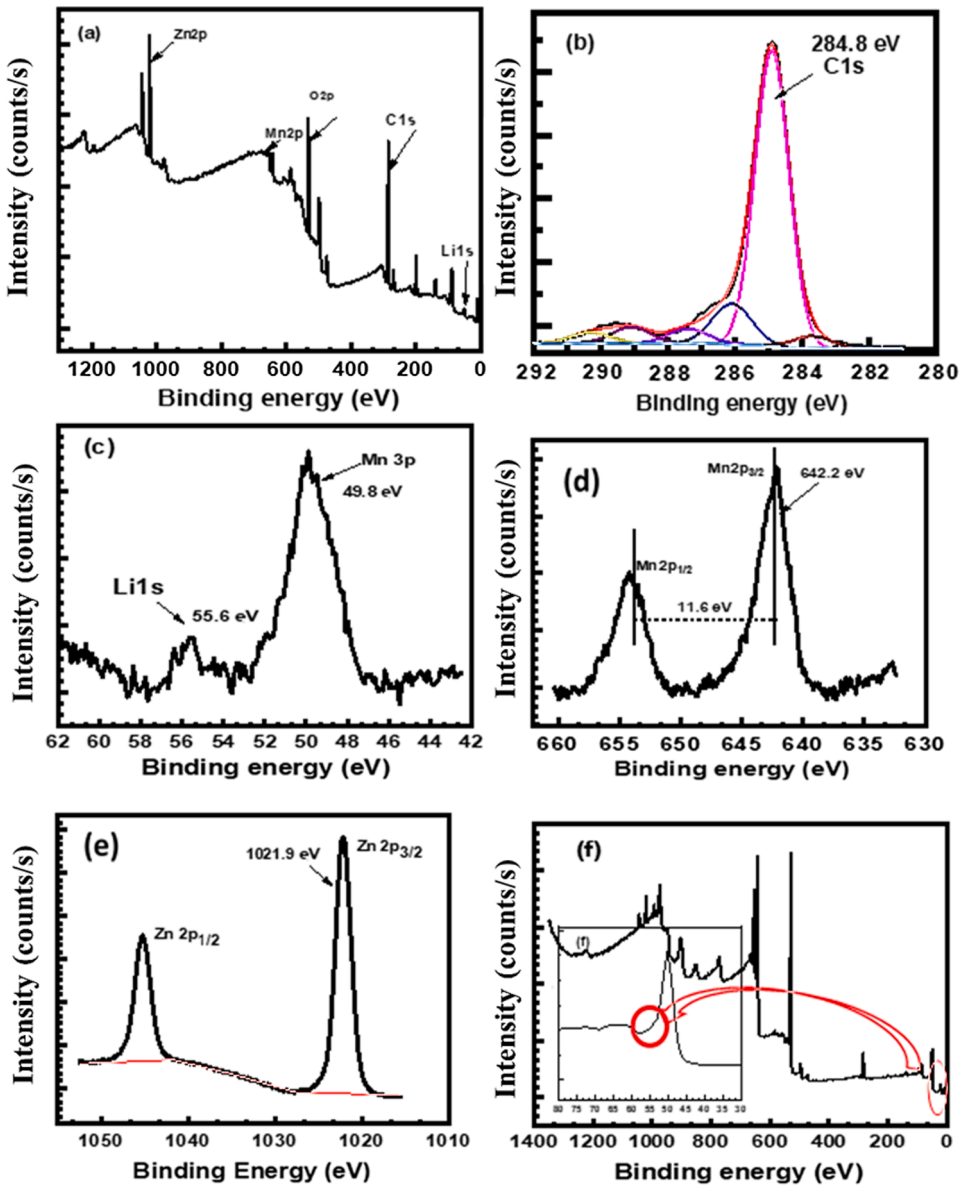

Fig. 4. XPS Studies: (a) General survey scan of $LiMn_2O_4$: Zn (b) C1s spectra (c) High resolution spectra Li 1s & Mn 3p (d) Mn 2p spectra (e) Zn 2p spectra, (f) XPS general survey for protonated HMn_2O_4: Zn, No Li identified at around 55 eV (see inset).

Adsorption is regarded as one of the most effective, economical, adaptable, and simple-to-control techniques for water and wastewater purification among all of the approaches mentioned above. In many instances, the adsorbent is inexpensive and doesn't require preparation before use. Hence, ecologists throughout the world frequently use the adsorption technique to remove harmful and poisonous inorganic and organic contaminants from water. It is frequently the finest option for wastewater treatment. Like other treatment methods, Adsorption does create a substance that can be difficult to dispose of properly. Adsorption is one of the most effective techniques among all the traditional ways since it has the potential for regeneration, recovery, and recycling of adsorbents in addition to being environmentally benign, economical, and effective at removing dyes on a big scale. It is often used to extract pollutants by causing them to be attached to adsorbents. Many kinds of adsorbents were reported for the consecutive removal of dyes from wastewater earlier, For example, Modified clay as adsorbent for the removal of basic red 46 and reactive yellow 181 [15], Chitosan-derived adsorbent reported for the removal of Methylene blue [16], biosorbent derived from Malaysian durian seeds for the removal of a Crystal violet [17], biosorbent derived from Hyacinth and Tinospora cordifolia plants for removal of Methyl red from wastewater [18], Microalgae for the removal of Crystal violet and Methylene blue [19], Zeolites synthesized from fly ash as an effective adsorbent for the removal of Methylene blue [20], ZnAl/NiAl-Magnetite humic acid for adsorption of Congo red from aqueous solution [21], Charcoal activated as template Mg/Al layered double hydroxide for selective adsorption of Direct yellow [22]. Metal oxides, among the different adsorbents available, have potential applications in water treatment due to their large surface area and inexpensive production and regeneration costs [23]. Various metal oxides have been already reported for the removal of different sorts of dyes [24–26]. Due to interesting properties like recyclability, meticulous morphology, structure stability, plentiful availability, and flexible surface chemistry along with outstanding mechanical, thermal, and optical properties of transition metal doped metal oxides make them supreme adsorbents for dye degradation [27–30]. Previously Protonated forms of Lithium manganese oxides have been reported for wastewater treatment [31]. Due to the greater solubility of manganese from lithium manganese oxide after acid treatment, long-term lithium extraction/insertion cycles

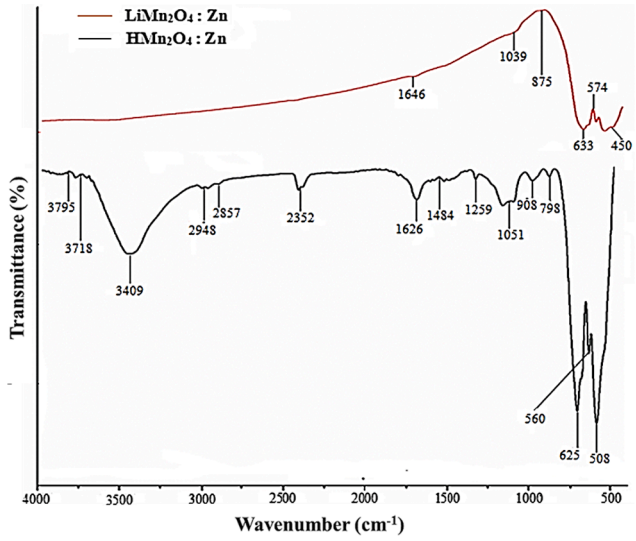

Fig. 5. FTIR of $LiMn_2O_4$: Zn and HMn_2O_4: Zn.

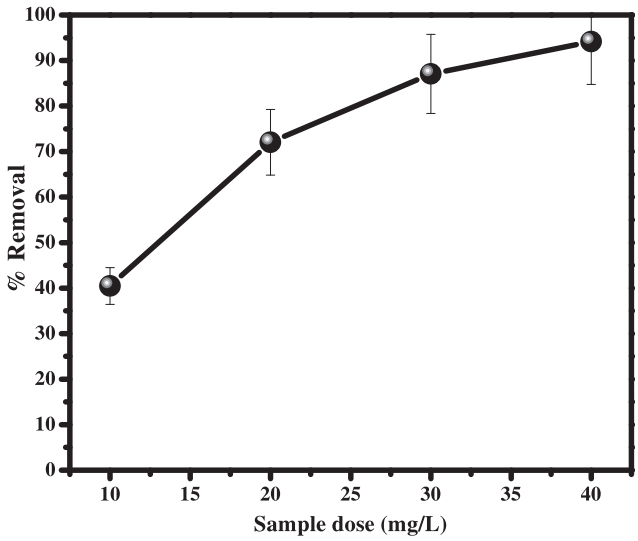

Fig. 7. The adsorption capacity of HMn_2O_4: Zn nano sorbent.

Table 1
CHNS analysis of $LiMn_2O_4$: Zn and HMn_2O_4: Zn.

Elements	$LiMn_2O_4$: Zn	HMn_2O_4: Zn
C	0.000	0.000
H	0.057	0.246
N	0.000	0.000
S	0.000	0.000

Table 2
BET surface analysis of HMn_2O_4: Zn.

BET surface area (m^2/g)	85.000
Total pore volume (cm^3/g)	0.206
Pore diameter (nm)	8.748

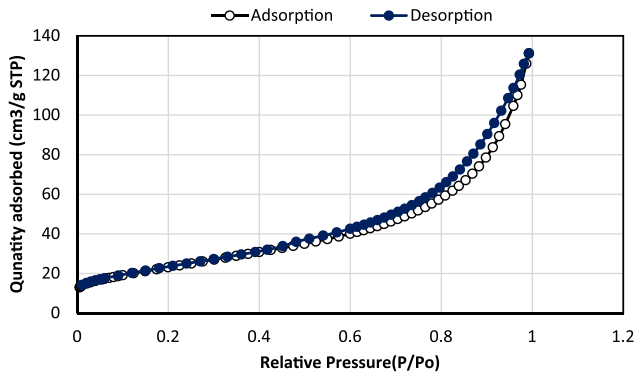

Fig. 6. BET Analysis HMn_2O_4: Zn.

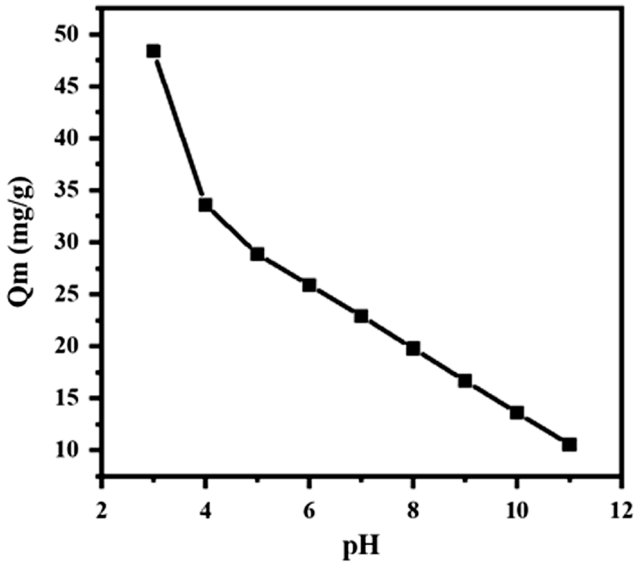

Fig. 8. Effect of solution pH on methyl orange adsorption by HMn_2O_4: Zn nano sorbent.

may be reduced. Following a thorough review of the literature, it can be determined that metal-doped lithium manganese oxide can increase structural stability by establishing a strong bond between the doped metal and oxygen, preventing manganese from dissolving in the solution [32]. Many different types of transition metal doped metal oxides have been proven to degrade dyes [33–35].

Several methods can be used to make metal-doped metal oxides with various combinations. Copper-doped manganese oxides by the solvothermal method [36], cobalt-doped manganese oxides by the facile inverse micelle sol–gel method [37], iron-doped manganese oxides by the solid-state method [38]. For the effective removal of various contaminants, the use of nano-adsorbents in wastewater treatment is a good strategy. Researchers have recently looked into the possibility of nano-adsorbents. The efficacy of NPs used as adsorbents is influenced by a variety of parameters, including surface chemistry, size, shape, fractal dimension, solubility, chemical content, and structure. Due to small particle size, their chemical activity and adsorption capacity increase [39]. magnesium doped lithium manganese oxides nanosorbent by single-step synthesis previously reported for removal of heavy metals [40].

In the present work, a single-step calcination method for the preparation of zinc-doped lithium manganese oxides nano sorbent is reported. The further protonated form of zinc-doped lithium manganese oxides prepared for superior performance in the adsorption of methyl orange dye. The Effect of different parameters like pH, contact time, and dosage were analyzed on the adsorption of methyl orange. Langmuir and Freundlich adsorption models as well as Pseudo first order, Pseudo second order, and intra-particle diffusion kinetic models were applied to evaluate the adsorption efficiency and process.

2. Methods and material

2.1. Materials

For the synthesis of zinc-doped lithium manganese oxides Sdfine analytical reagent grade extra pure lithium chloride (99 %), lithium carbonate (99 %), and zinc acetate dihydrate (98 %) were bought and utilized as it is. Manganese acetate tetrahydrate (99 %) was purchased from Finar Chemical AR grade. Hydrochloric acid (95 %) and Methyl orange were procured from Merck chemicals.

2.2. Synthesis of novel zinc-doped lithium manganese oxides nano sorbent

Zinc-doped Lithium manganese oxide (0.4/1.6 M ratio of Zn/Mn) was prepared by making a eutectic mixture of 447 mg Lithium carbonate, 342 mg Lithium chloride, 6931 mg Manganese acetate tetrahydrate, and 2687 mg of Zinc acetate dihydrate by grinding them in Mortar pestle for 30 min. This fine mixture was placed in an Alumina crucible and dried the mixture for 8 h in the oven (Yorco) at 100 °C. After that, the mixture was calcined in a muffle furnace at 500 °C for 5 h. The product was washed 4–5 times with double distilled water and dried at 90 °C.

2.3. Protonation of zinc-doped lithium manganese oxides nano sorbent

Add 150 mL of 0.5 M HCl to 2.0 gm fine powder of Zn-doped Lithium manganese oxide. The HMn_2O_4: Zn sample combination was allowed to stand for 24 h in a stirring condition for protonation. After agitating the mixture for 24 h, the sample particles settled down, the HCl was decanted, and the sample was thoroughly washed with double distilled water for 3–4 times. The sample was then dried in an oven at 80 °C for 7–8 h.

The possible reaction under temperature-induced chemical synthesis is given as follows,

$$\underset{\text{Molten salt}}{LiCl + Li_2CO_3 + Mn(COO)_2.4H_2O + Zn(COO)_2.2H_2O} \longrightarrow LiZn_xMn_{2-x}O_4 + H_2O + CO_2 + CO + CH_3COCH_3$$

$$(X = 0.4)$$

$$LiZn_xMn_{2-x}O_4 + HCl \longrightarrow HZn_xMn_{2-x}O_4 + LiCl$$

2.4. Characterization

Powder X-ray Diffraction was performed for phase identification and indexing of the product by BRUKER D8 diffractometer using Cu Kα irradiation (λ = 1.54060 \AA). FTIR was made using a Perkin Elmer Spectrum FTIR spectrometer by the KBr pellet method. Elemental analysis was done by using ELEMENTAR MODEL VARIO MICRO TUBE to identify that protonation was done successfully. BET analysis was executed to determine the surface Area, pore size, and pore volume from nitrogen adsorption/desorption isotherm at −195 °C by using a MICROMERITICS 3Flex Version 4.03. HRTEM images were attained by JEOL JEM 2100. XPS analysis made by thermo-scientific NEXSA by using low energy (1486.6 eV) X-rays (Al K-α). pH adjustment was done with EUTECH instruments pH tutor. The adsorption study was performed at 461 nm by using SYSTRONICS DOUBLE BEAM UV–VIS SPECTROPHOTOMETER 2201 having a 3 nm bandwidth.

2.5. Adsorption studies

The adsorption study was carried out by preparing a 1000 mg/L stock solution of standard methyl orange in deionized water. The further diluted solution was directly used for the same. The whole study was performed at room temperature. The effect of contact time was performed by adding 5 mg of adsorbent in 25 mL of methyl orange. Measure the absorbance of filtrate at 0–6 h of stirring in UV at 461 nm. The effect of pH on MO adsorption was investigated using a pH range of 3–11 and a starting concentration of 1 mg/L methyl orange. 0.1 M HCl and NaOH were used to alter the pH of the solution.

The effect of dosage was tested using different amounts of adsorbent (1–4 gm/L) in a 10 ppm methyl orange solution. The content was filtered after 6 h of continuous stirring, and the absorbance was measured in UV at 461 nm. The amount of MO adsorbed on the adsorbents was calculated by the following equation (1).

$$Q_e = \frac{(C_i - C_e)V}{W} \quad (1)$$

$C_i = Initial\ concentration\ MO$

$C_e = final\ concentration\ MO$

$V = Volume\ of\ solution$

$W = Weight\ of\ adsrobent$

2.6. Reusability of nanosorbents

To evaluate the reusability of the nanosorbent, the adsorbed methyl orange was removed from the nanosorbent by dissolving it in a methanol solution. Then nanosorbent was washed with plenty of deionized water and charged the nanosorbent by using 0.5 M HCl. Adsorption- desorption cycle was performed four times to study the influence of recyclability. Recycled nanosorbent are utilized for different studies.

3. Result and discussion

3.1. Characterization

3.1.1. Crystal structure by using X-ray diffraction

The Crystalline structure of Zinc doped lithium manganese oxides was identified by appeared diffraction peaks at (111), (200), (112), (031), (311), (211), (140), (012), (212), (222), (160), (331), (340), (400) crystallographic plans with the space group of Fd-3m (JCPDS no. 33-0803) which shows in Fig. 1. The observed high intense peak indicates a well-crystalline phase of lithium manganese oxides followed by thermally induced synthesis [41,42]. However, Fig. 2b shows a diffraction profile for the HMn_2O_4: Zn. Some of the peaks that disappear in the protonated sample may be due to the dissolution of metal oxides during the protonation mechanism. Both materials were synchronized with a cubic structure having Fd-3m space group, in which tetrahedral sites occupied lithium ions and octahedral sites occupied for manganese ions. The average crystalline size was calculated a 26 nm for zinc-doped lithium manganese oxides and 25 nm for protonated by using the

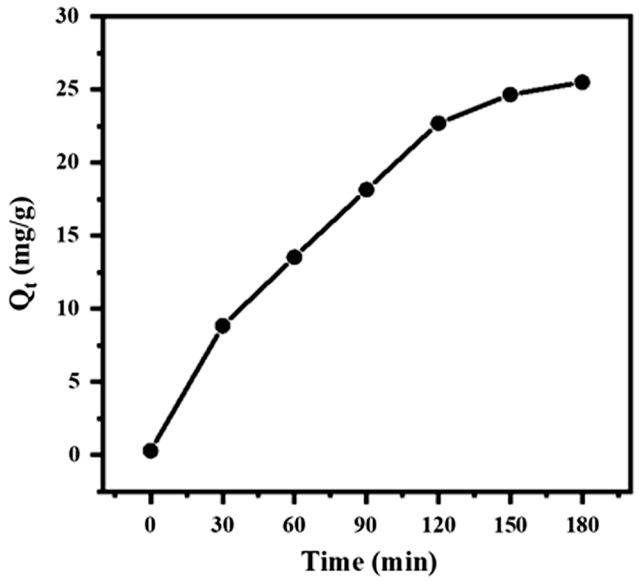

Fig. 9. Effect of contact time on Methyl Orange adsorption by HMn_2O_4: Zn nano sorbent. (For interpretation of the references to colour in this figure legend, the reader is referred to the web version of this article.)

Scherrer equation.

3.1.2. Morphological studies: High-resolution transmission electron microscope analysis

The morphological investigations of the $LiMn_2O_4$: Zn and HMn_2O_4: Zn nanostructures were analyzed by HR-TEM, Fig. 3a–f. The samples were dispersed in ethanol and carbon carbon-coated grid was used to analyze the samples. The fine spherical shaped nanomaterials were observed in the case of $LiMn_2O_4$: Zn sample with 14.3 nm average sizes Fig. 3a–c. However, the aggregated nanostructures appeared in the case of HMn_2O_4: Zn which has 13 nm of average size Fig. 3d–f.

3.1.3. X-ray photoelectron spectroscopy analysis

XPS analysis of the as-prepared samples has been done to investigate the oxidation states of the expected elements such as Li, Zn, and Mn into the $LiMn_2O_4$: Zn compound. The charge of the carbon peak has been - corrected to the standard value of 284.8 eV binding energy. Fig. 4 shows the XPS spectra of the Zn-doped Lithium manganese oxides. [43]. The XPS survey scan displays all the expected peaks like C, N, Li, Mn, and Zn with correspond to their binding energies (Fig. 4a). The peak at 55.6 eV indicates the presence of Li metal while the Mn 3p showed a clear peak at 49.8 eV binding energy (Fig. 4c). Again a high resolution of Mn spectra was analyzed to confirm the oxide state of the Mn. The peak at around 642.2 eV indicates that Mn is present in the form of Mn_2O_4 as it has 11.6 eV differences between splitting states of Mn 2p (Fig. 4d). [44]. Furthermore, the metallic Zn element confirmed in $LiMn_2O_4$: Zn by the presence of Zn 2p peak at 1021.9 eV binding energy. So, by the XPS analysis, the oxidation states of the metals and metal-oxides have been confirmed in $LiMn_2O_4$: Zn while there is no evidence of Li in protonated sample around 55.6 eV binding energy (Fig. 4f).

3.1.4. Bonding characteristics and elemental analysis by FTIR and CHNS analyzer

Fourier-transform infrared (FT-IR) spectra for $LiMn_2O_4$: Zn and HMn_2O_4: Zn samples are shown in Fig. 5. The FTIR bands at about 615 and 513 cm^{-1} can be attributed to the asymmetric stretching of the Mn—O [45]. IR frequencies 458, 508, and 574 cm^{-1} are ascribed to the Zn—O bond [46]. IR band at 908 cm^{-1} assigned to Zn-OH bond [47]. IR band at 3409 cm^{-1} indicates O—H stretching of the hydroxyl group due to bounded water [33]. IR band observed at 1484 is accredited to the characteristic stretching band of a carbonate attached to the nano-structure [48].

Protonation was made successfully, which was confirmed from the elemental (C, H, N, S) analysis. Zero results for carbon, nitrogen, and sulphur, before and after acid wash which confirmed that there are no impurities present in products (Table 1).

3.1.5. Surface area measurement by using BET analysis

BET analysis plays a vital part in the material's photocatalytic performance. Indeed, the adsorption of organic pollutants in wastewater on the photo catalyst's surface is an important stage in the remediation of organic pollutants. Table 2 shows various parameters related to the BET analysis. Moderate surface area of the synthesized nanocatalysts which is higher than the typical threshold for low surface area and it is may be due to the unique porous networks and complex structure of material [45]. N_2 adsorption–desorption isotherms with corresponding surface area and pore size of the protonated form of Zn doped lithium manganese oxides were investigated and type II isotherms were presented in

Table 3
Langmuir and Freundlich isotherm parameters of nanosorbents.

Isotherm	Parameter	Value
Langmuir	Q_{max}	312.500 mg/g
	K_L	0.091 L/mg
	r^2	0.957
	R_L	0.099–0.354
Freundlich	K_f	37.150 mg/g
	n	1.792
	r^2	0.926

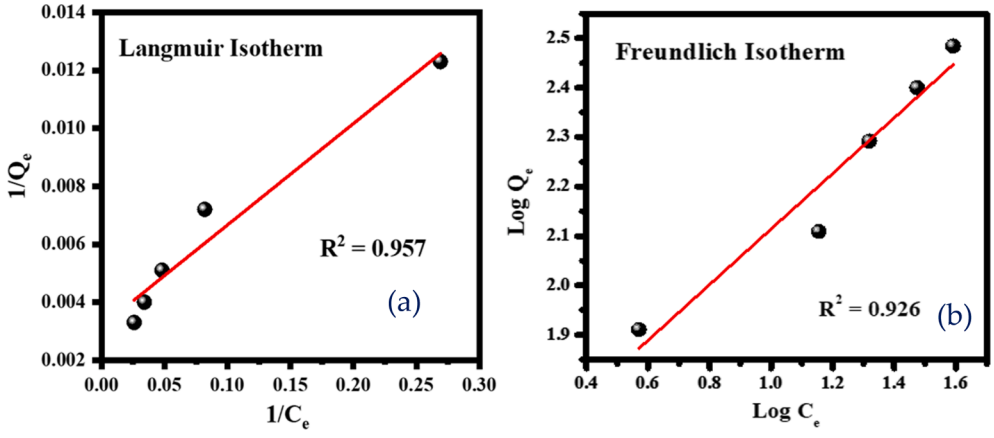

Fig. 10. (a) Langmuir and (b) Freundlich Isotherms.

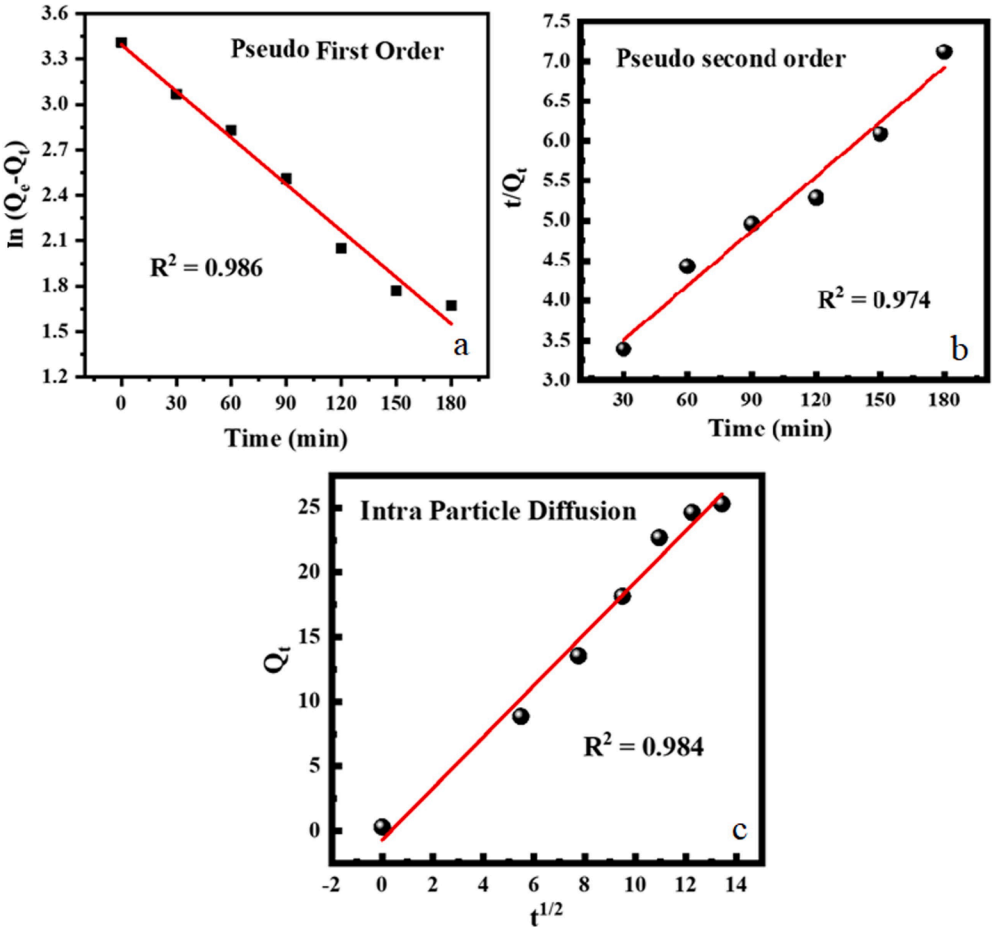

Fig. 11. Kinetic study of nano sorbent (a) Pseudo first order (b) Pseudo second order (c) Intra particle diffusion.

Table 4
Kinetics parameter of nano sorbent.

Kinetic	Parameter	MO
Pseudo First Order	Q_e(mg/g)	30.147
	k_1(min^{-1})	5.833 * 10^{-5}
	R^2	0.986
Pseudo Second order	Q_e(mg/g)	43.859
	k_2(g/mg. Min)	0.184 * 10^{-3}
	R^2	0.974
Intra Particle diffusion	k_{id}(mg/g. min$^{3/2}$)	0.493
	C(mg/g)	0.474
	R^2	0.984

Fig. 6 which represents monolayer–multilayer adsorption obtained with macroporous adsorbent.

3.2. Adsorption studies

Fig. 7 shows the adsorption capacity of nano sorbent doses (10, 20, 30, 40 mg/L) was observed for the removal of methyl orange with an initial concentration of 10 ppm. The % removal of methyl orange is found to increase with the increase in adsorbent amount due to increased sites of nano sorbent. Almost 40.48, 72.02, 87.05, and 94.16 % removal of methyl orange was achieved with 0.1, 0.2, 0.3, and 0.4 gm/L dose of nano sorbent respectively.

The pH of the solution plays a significant role in the adsorption study of dyes as adsorptive capacity and ionization or dissociation of adsorbate molecules as well as influence on the surface properties of the adsorbent. The effect of pH on adsorption was examined in the pH range from 3 to 11. Fig. 8 shows that MO adsorption ability decreases with an increase (3–11) in the pH of a solution. Improved adsorption ability is assumed due to strong electrostatic attraction between positively charged surfaces and anionic MO species at lower pH, the surfaces of adsorbent materials were positively charged due to protonation. The coulomb repulsion between the negatively charged surfaces and the dye molecules increased as the pH value (basic conditions) increased. Lower adsorption of MO at high pH may be due to the presence of hydroxide ions in the solution [49–51].

The equilibrium time of adsorbent with pollutants is a key parameter in the progression of dye adsorption from wastewater. The study was carried out with an Initial concentration of 10 mg/L of methyl orange by keeping an identical amount of adsorbents at room temperature. From the study, it was found that 3 h of contact time is sufficient to achieve equilibrium. The effect of the contact time of adsorbent with methyl orange is shown in Fig. 9. This shows that the adsorption of methyl orange at the initial time interval was found rapid due to having a large number of vacant sites on the surface of the adsorbent. Conversely, a plateau is constant after a certain interval of time, which shows that the adsorption of methyl orange by Nanosorbent has reached its equilibrium stage due to less number of vacant sites remaining for adsorption and repulsive forces between MO and adsorbent increases [6].

3.2.1. Adsorption isotherm- Langmuir and Freundlich isotherm

Isotherm models were used to assess the maximum adsorptive capacity of the adsorbent as well as the nature of the interactions between the nanosorbent and dye species[52]. There are two most useful isotherm models Langmuir and Freundlich, were applied for the explanation of the solid–liquid adsorption system. Langmuir model is

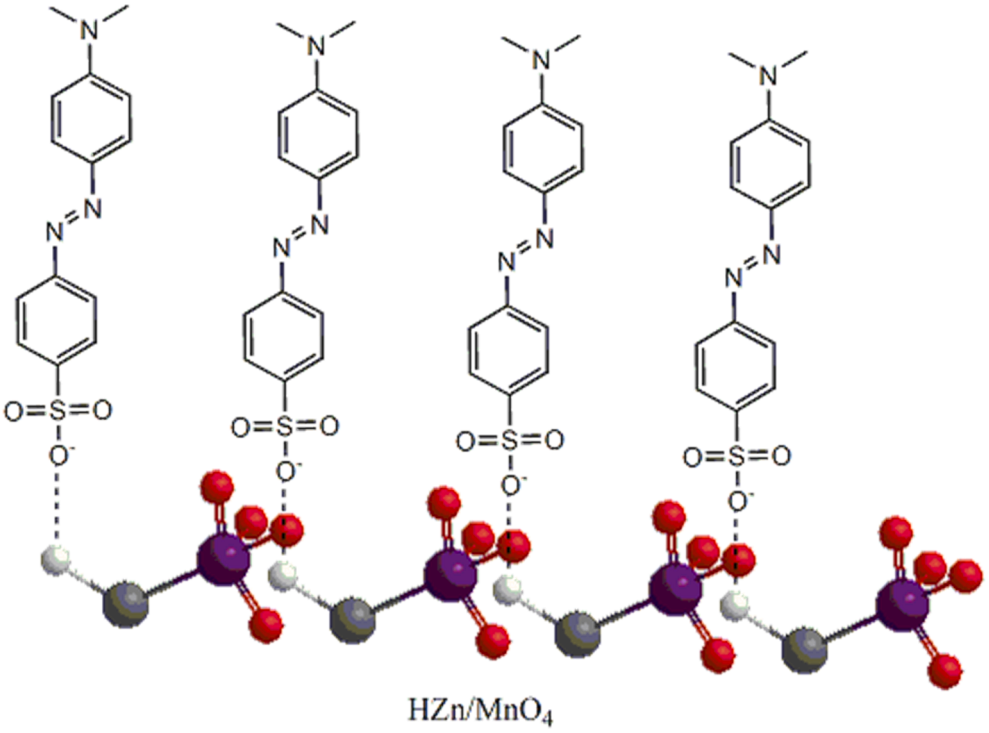

Fig. 12. Feasible electrostatic interaction between positively charged nanosorbent and negatively charged MO.

Table 5
Comparison of methyl orange adsorption efficiency on synthesized nanosorbent with other adsorbents.

Adsorbents	Q_{max}(mg/g)	pH	T (°C)	Method for evaluation of Q_{max}	Ref.
AC from sugarcane mills boiler residue	161.80	5.0	25.0	Langmuir	[60]
Coffee waste/cetyl pyridinium chloride and Coffee waste/cetyl trimethyl ammonium bromide	62.50 58.82	3.5 3.5	25.0 25.0	Langmuir	[61]
Activated biochar from pomelo peel waste	163.10	3.0	25.0	Langmuir	[62]
Cd-zeolite imidazolate framework (Cd-ZIF-8)	145.50	2.0	50.0	Langmuir	[63]
Polyvinylidene fluoride/PEDOT mats	146.20	3.0	20.0	Langmuir	[64]
p-CNTs/N, N-diethyl ethanol ammonium chloride	263.10	2.0	–	Langmuir	[65]
Mesoporous MCM-41/microfiltration membrane	151.50	4.0	25.0	Langmuir	[66]
ZIF-67 nanostructure	75.59	–	–	Langmuir	[67]
Chitosan/H_2O_2 activated anthracite	297.30	3.0	25.0	Langmuir	[68]
Polydopamine/ polyethylene mine/ graphene oxide	237.50	–	40.0	Langmuir	[69]
La/Co modified sugar-based carbon	285.10	6.5	–	Langmuir	[54]
Zinc-doped lithium manganese oxides nano sorbent	312.50	3.0	25.0	Langmuir	Existent study

validated for mono-layer adsorption on effortlessly homogeneous and smooth surfaces. Conversely, the Freundlich model is validated for Multilayer adsorption on heterogeneous surfaces [53,54].

Langmuir adsorption can be expressed by the following equation.

$$\frac{1}{Qe} = \frac{1}{K_L\, Q_{max}} \bullet \frac{1}{C_e} + \frac{1}{Q_{max}}, \tag{2}$$

Where Qe (mg/g) is the amount of dye adsorbed per unit mass of the adsorbent at the equilibrium point, C_e (mg/L) is the concentration of dye after equilibrium, Q_{max} (mg/g) is the maximum amount of adsorbate and K_L (L/mg) is the Langmuir constant. The value of Q_{max} and K_L can be determined from the slope and intercept value of the graph $\frac{1}{Qe}$ vs. $\frac{1}{C_e}$ presented in Fig. 10(a). The parameter that defines the adsorption system is favorable or not i.e. R_L is called the separation factor or equilibrium parameter. It can be used to describe the efficiency of the adsorption $R_L = \frac{1}{1+C_i * K_L}$, R_L indicate the isotherm shapes which can be unfavorable ($R_L > 1$), linear ($R_L = 1$), favorable ($0 < R_L < 1$), or irreversible ($R_L = 0$). As shown in (Table 3), the R_L values were found to be in the 0.099–0.354 range, indicating that the adsorption of MO is favorable.

And Freundlich adsorption can be explained by the following equation.

$$LogQe = LogK_f + \frac{1}{n} LogCe \tag{3}$$

Where Qe (mg/g) is the amount of dye adsorbed per unit mass of the adsorbent at the equilibrium point, C_e (mg/L) is the concentration of dye after equilibrium, K_f represents adsorption capacity, and n represents the adsorption efficiency are the Freundlich constant which can be calculated from the slope and intercept value of Linear plot $LogQe$ vs. $LogCe$ presented in Fig. 10(b). Adsorption is favorable if the value of n lies between the ranges of 1–10 (see Fig. 11).

In adsorption studies, R^2 values are a useful tool for evaluating the goodness of fit between experimental data and isotherm models[55]. The monolayer adsorption process on a positively charged homogenous surface is attributed to the Langmuir isotherm, which is closely matched

with good correlation coefficients (near 1) compared to the Freundlich isotherm according to the characteristics presented in (Table 3).

3.2.2. Adsorption kinetics

Kinetic studies are indispensable for unraveling the adsorption mechanism by providing valuable information about the rate of adsorption, mechanisms, controlling steps, and the interactions involved [56,57]. Three kinetics models i.e. Pseudo first order, Pseudo second order, and intra-particle diffusion were applied to understand the adsorption process of nano sorbent. Equations (4)–(6), which represent the linear equation forms of the PFO, PSO, and IPD, respectively, are used to compute the kinetic parameters[58].

$$ln(Q_e - Q_t) = lnQ_e - \frac{k_1 t}{2.303} \quad (4)$$

Where Q_e and Q_t are the amounts of MO adsorbed (mg/g) at equilibrium and at time t (min), respectively, k_1 (min^{-1}) is the rate constant of the pseudo-first-order kinetic model

$$\frac{t}{Qt} = \frac{1}{k_2 * Q_e^2} + \frac{t}{Q_e}, \quad (5)$$

Where k_2 is the rate constant (g/mg. min) of the pseudo-second-order kinetic model for adsorption.

$$Q_t = k_{id} t^{\frac{1}{2}} + C, \quad (6)$$

Where k_{id} is the intra-particle diffusion rate constant (mg/g. $min^{3/2}$) and the values of C (mg/g) depict the boundary thickness.

Table 4 shows the kinetic parameters of the nano sorbent for methyl orange. The highest R^2 value correlated with PFO is closer to unity over the PSO and IPD model (Fig. 12). The findings presented here provide evidence that the MO adsorb on nanosorbent through physisorption as a rate-limiting step, which includes electrostatic attraction[59].

To understand the interaction between positively charged nano-sorbent and negatively charged MO, an electrostatic interaction is shown in Fig. 12. Structurally negative sites of the dye molecules interact with the positive groups of the synthesized absorbent (HZn/Mn_2O_4) which enhances the adsorption strength on the surface of the used catalysts.

Positively charged zinc-doped lithium manganese oxides are attained by modifying the surface of zinc-doped lithium manganese oxide using a protonation mechanism with hydrochloric acid, which is established by elemental analysis, XRD, and FTIR. Electrostatic forces, which are produced by the attraction between the positively charged surface of nanosorbent and the negatively charged MO is the main mechanism causing the adsorption of MO on it, as illustrated in Fig. 12.

(Table 5) shows a comparison of methyl orange adsorption efficiency on synthesized nano sorbent with other adsorbents.

4. Conclusion

In this work, a Zinc-doped lithium manganese oxides ($LiZn_xMn_{2-x}O_4$, where x = 0.4) nanosorbents have been synthesized by using an optimized calcination method. Structural characterization made with XRD, TEM, XPS, FTIR, and the protonation was confirmed by the CHNS analyzer. The 14.3 and 13 nm particle sizes for $LiMn_2O_4$: Zn and HMn_2O_4: Zn were confirmed by TEM analysis. Metallic Zn element confirmed in $LiMn_2O_4$: Zn by the presence of Zn 2p peak at 1021.9 eV binding energy. The experimental data of adsorption isotherm are found to be best fitted to the Langmuir model compared to the Freundlich model, and its correlation coefficient is relatively close to unity. The highest R^2 value correlated with PFO is closer to unity over PSO and IPD models. The findings presented here provide evidence that the MO adsorb on nanosorbent through physisorption as a rate-limiting step, which includes electrostatic attraction. Kinetic data attributes that MO adsorption follows Pseudo-first-order adsorption. HMn_2O_4: Zn showed good adsorption capacities of 312 mg/g and showed almost 94.16 % removal of dye (methyl orange).

CRediT authorship contribution statement

Pooja R. Popat: Conceptualization, Data curation, Formal analysis, Investigation, Methodology, Project administration, Validation, Visualization, Writing – original draft, Writing – review & editing. **Abeer Yousef Alyami:** Writing – original draft. **Gajendra Kumar Inwati:** Data curation, Writing – original draft, Writing – review & editing. **Bharat A. Makwana:** Conceptualization, Investigation, Methodology, Project administration, Resources, Supervision, Validation, Visualization, Writing – original draft, Writing – review & editing. **Maha Awjan Alreshidi:** Writing – original draft, Writing – review & editing. **Jari S. Algethami:** Investigation, Software, Visualization, Writing – original draft, Writing – review & editing. **Mohamed Abbas:** Formal analysis, Validation, Visualization, Writing – original draft, Writing – review & editing. **Krishna Kumar Yadav:** Resources, Writing – original draft.

Declaration of competing interest

The authors declare that they have no known competing financial interests or personal relationships that could have appeared to influence the work reported in this paper.

Data availability

The authors do not have permission to share data.

Acknowledgments

The authors extend their appreciation to the Deanship of Scientific Research at King Khalid University (KKU) for funding this research through the Research Group Program Under the Grant Number:(R.G. P.2/572/44). The authors are thankful to the Deanship of Scientific Research at Najran University for funding this work under the Research Groups Funding program grant code (NU/RG/ SERC/12/45).

References

[1] A.A. Inyinbor, O.S. Bello, A.P. Oluyori, H.E. Inyinbor, A.E. Fadiji, Wastewater conservation and reuse in quality vegetable cultivation: overview, challenges and future prospects, Food Control 98 (2019) 489–500.
[2] D. Baskar, A.K. Selvam, M. Ganesan, G. Nallathambi, Mechanism of nanofibres on removal of water pollutants-a review (2018).
[3] M.E. El-Sayed, Nanoadsorbents for water and wastewater remediation, Sci. Total Environ. 739 (2020) 139903.
[4] A.H. Jawad, B. Hameed, A.S. Abdulhameed, Synthesis of biohybrid magnetic chitosan-polyvinyl alcohol/MgO nanocomposite blend for remazol brilliant blue R dye adsorption: solo and collective parametric optimization, Polym. Bull. 80 (2023) 4927–4947.
[5] M. Shariati-Rad, M. Irandoust, S. Amri, M. Feyzi, F. Ja'fari, Removal, preconcentration and determination of methyl red in water samples using silica coated magnetic nanoparticles, J. Appl. Res. Water Wastewater 1 (2014) 6–12.
[6] A. Mittal, A. Malviya, D. Kaur, J. Mittal, L. Kurup, Studies on the adsorption kinetics and isotherms for the removal and recovery of Methyl Orange from wastewaters using waste materials, J. Hazard. Mater. 148 (2007) 229–240.
[7] A. Darwish, M. Rashad, H.A. AL-Aoh, Methyl orange adsorption comparison on nanoparticles: isotherm, kinetics, and thermodynamic studies, Dyes Pigm. 160 (2019) 563–571.
[8] A. Fetimi, A. Dâas, S. Merouani, A.M. Alswieleh, M. Hamachi, O. Hamdaoui, O. Kebiche-Senhadji, K.K. Yadav, B.H. Jeon, Y. Benguerba, Predicting emulsion breakdown in the emulsion liquid membrane process: optimization through response surface methodology and a particle swarm artificial neural network, Chem. Eng. Process.-Process Intensif. 176 (2022) 108956.
[9] C. Li, T. Lou, X. Yan, Y.-Z. Long, G. Cui, X. Wang, Fabrication of pure chitosan nanofibrous membranes as effective absorbent for dye removal, Int. J. Biol. Macromol. 106 (2018) 768–774.
[10] Y.-Y. Lau, Y.-S. Wong, T.-T. Teng, N. Morad, M. Rafatullah, S.-A. Ong, Degradation of cationic and anionic dyes in coagulation–flocculation process using bi-functionalized silica hybrid with aluminum-ferric as auxiliary agent, RSC Adv. 5 (2015) 34206–34215.

[11] W. Chen, J. Mo, X. Du, Z. Zhang, W. Zhang, Biomimetic dynamic membrane for aquatic dye removal, Water Res. 151 (2019) 243–251.
[12] K. Dutta, S. Mukhopadhyay, S. Bhattacharjee, B. Chaudhuri, Chemical oxidation of methylene blue using a Fenton-like reaction, J. Hazard. Mater. 84 (2001) 57–71.
[13] S. Rajendran, G.K. Inwati, V.K. Yadav, N. Choudhary, M.B. Solanki, M. H. Abdellattif, K.K. Yadav, N. Gupta, S. Islam, B.-H. Jeon, Enriched catalytic activity of TiO2 nanoparticles supported by activated carbon for noxious pollutant elimination, Nanomaterials 11 (2021) 2808.
[14] L. Dai, W. Zhu, L. He, F. Tan, N. Zhu, Q. Zhou, M. He, G. Hu, Calcium-rich biochar from crab shell: an unexpected super adsorbent for dye removal, Bioresour. Technol. 267 (2018) 510–516.
[15] F. Bouatay, S. Dridi-Dhaouadi, N. Drira, M. Farouk Mhenni, Application of modified clays as an adsorbent for the removal of Basic Red 46 and Reactive Yellow 181 from aqueous solution, Desalin. Water Treat. 57 (2016) 13561–13572.
[16] A. Salama, P. Hesemann, New N-guanidinium chitosan/silica ionic microhybrids as efficient adsorbent for dye removal from waste water, Int. J. Biol. Macromol. 111 (2018) 762–768.
[17] A. Fetimi, S. Merouani, M.S. Khan, M.N. Asghar, K.K. Yadav, B.H. Jeon, M. Hamachi, O. Kebiche-Senhadji, Y. Benguerba, Modeling of textile dye removal from wastewater using innovative oxidation technologies (Fe (II)/chlorine and H2O2/periodate processes): artificial neural network-particle swarm optimization hybrid model, ACS Omega 7 (16) (2022) 13818–13825.
[18] K.V. Ramana, K.S. Latha, K. Ravindranath, B.H. Babu, Methyl red dye removal using new bio-sorbents derived from hyacinth and tinospora cordifolia plants from waste waters, Rasāyan J. Chem. 10 (2017) 349–362.
[19] A.S. Abdulhameed, A.H. Jawad, E. Kashi, K.A. Radzun, Z.A. ALOthman, L. D. Wilson, Insight into adsorption mechanism, modeling, and desirability function of crystal violet and methylene blue dyes by microalgae: Box-Behnken design application, Algal Res. 67 (2022) 102864.
[20] W. Chunfeng, L. Jiansheng, W. Lianjun, S. Xiuyun, J. Huang, Adsorption of dye from wastewater by zeolites synthesized from fly ash: kinetic and equilibrium studies, Chin. J. Chem. Eng. 17 (2009) 513–521.
[21] N. Ahmad, F.S. Arsyad, I. Royani, P.M.S.B.N. Siregar, T. Taher, A. Lesbani, High regeneration of ZnAl/NiAl-Magnetite humic acid for adsorption of Congo red from aqueous solution, Inorg. Chem. Commun. 150 (2023) 110517.
[22] N. Ahmad, F.S. Arsyad, I. Royani, A. Lesbani, Charcoal activated as template Mg/Al layered double hydroxide for selective adsorption of direct yellow on anionic dyes, Results Chem. 5 (2023) 100766.
[23] M.A. Islam, I. Ali, S.A. Karim, M.S.H. Firoz, A.-N. Chowdhury, D.W. Morton, M. J. Angove, Removal of dye from polluted water using novel nano manganese oxide-based materials, J. Water Process Eng. 32 (2019) 100911.
[24] O.A. Oyewo, E.E. Elemike, D.C. Onwudiwe, M.S. Onyango, Metal oxide-cellulose nanocomposites for the removal of toxic metals and dyes from wastewater, Int. J. Biol. Macromol. (2020).
[25] H.J. Ahn, Y. Ahn, M.B. Kurade, S.M. Patil, G.S. Ha, P.O. Bankole, M.A. Khan, S. W. Chang, M.H. Abdellattif, K.K. Yadav, B.H. Jeon, The comprehensive effects of aluminum oxide nanoparticles on the physiology of freshwater microalga Scenedesmus obliquus and it's phycoremediation performance for the removal of sulfacetamide, Environ. Res. 215 (2022) 114314.
[26] L. Li, J. Xiao, P. Liu, G. Yang, Super adsorption capability from amorphousization of metal oxide nanoparticles for dye removal, Sci. Rep. 5 (2015) 1–6.
[27] W.R. Thalgaspitiya, T.K. Kapuge, J. He, B. Deljoo, A.G. Meguerdichian, M. Aindow, S.L. Suib, Multifunctional transition metal doped titanium dioxide reduced graphene oxide composites as highly efficient adsorbents and photocatalysts, Microporous Mesoporous Mater. 307 (2020) 110521.
[28] P. Ahuja, S.K. Ujjain, R. Kanojia, P. Attri, Transition metal oxides and their composites for photocatalytic dye degradation, J. Compos. Sci. 5 (2021) 82.
[29] F. Khurshid, M. Jeyavelan, S. Nagarajan, Photocatalytic dye degradation by graphene oxide doped transition metal catalysts, Synth. Met. 278 (2021) 116832.
[30] A. Rafiq, M. Imran, M. Aqeel, M. Naz, M. Ikram, S. Ali, Study of transition metal ion doped CdS nanoparticles for removal of dye from textile wastewater, J. Inorg. Organomet. Polym Mater. 30 (2020) 1915–1923.
[31] H. Park, N. Singhal, E.H. Jho, Lithium sorption properties of HMnO in seawater and wastewater, Water Res. 87 (2015) 320–327.
[32] R. Chitrakar, Y. Makita, K. Ooi, A. Sonoda, Magnesium-doped manganese oxide with lithium ion-sieve property: lithium adsorption from salt lake brine, Bull. Chem. Soc. Jpn. 86 (2013) 850–855.
[33] M. Siddique, N. Fayaz, M. Saeed, Synthesis, characterization, photocatalytic activity and gas sensing properties of zinc doped manganese oxide nanoparticles, Phys. B Condens. Matter 602 (2021) 412504.
[34] C. Boulechfar, H. Ferkous, S. Boufas, M. Berredjem, A. Delimi, S. Djellali, A. Djedouani, R. Bahadi, S. Laamari, K.K. Yadav, B.H. Jeon, Synthesis, electrochemical, and quantum chemical studies of some metal complexes: Mn (II), Co (II), and Zn (II) with 2-furaldehyde semicarbazone, J. Mol. Struct. 1271 (2023) 134007.
[35] S. Natarajan, H.C. Bajaj, Recovered materials from spent lithium-ion batteries (LIBs) as adsorbents for dye removal: equilibrium, kinetics and mechanism, J. Environ. Chem. Eng. 4 (2016) 4631–4643.
[36] X. Niu, Z. Lei, Copper doped manganese oxides to produce enhanced catalytic performance for CO oxidation, J. Environ. Chem. Eng. 7 (2019) 103055.
[37] H. Li, D. Chen, S. Li, C. Kang, Q. Liu, Synthesis of mesoporous cobalt-doped manganese oxides for high-performance supercapacitors, Ionics 27 (2021) 2181–2192.
[38] R. Chitrakar, Y. Makita, K. Ooi, A. Sonoda, Synthesis of iron-doped manganese oxides with an ion-sieve property: lithium adsorption from Bolivian brine, Ind. Eng. Chem. Res. 53 (2014) 3682–3688.
[39] K. Rouibah, H. Ferkous, A. Delimi, T. Himeur, M. Benamira, M. Zighed, A. S. Darwish, T. Lemaoui, K.K. Yadav, J.K. Bhutto, A. Ahmad, Biosorption of zinc (II) from synthetic wastewater by using Inula Viscosa leaves as a low-cost biosorbent: experimental and molecular modeling studies, J. Environ. Manage. 326 (2023) 116742.
[40] H. Saravaia, H. Gupta, P. Popat, P. Sodha, V. Kulshrestha, Single-step synthesis of magnesium-doped lithium manganese oxide nanosorbent and their polymer composite beads for selective heavy metal removal, ACS Appl. Mater. Interfaces 10 (2018) 44059–44070.
[41] S. Rajendran, S.G. Wanale, A. Gacem, V.K. Yadav, I.A. Ahmed, J.S. Algethami, S. D. Kakodiya, T. Modi, A.M. Alsuhaibani, K.K. Yadav, S. Cavalu, Nanostructured iron oxides: structural, optical, magnetic, and adsorption characteristics for cleaning industrial effluents, Crystals 13 (3) (2023) 472.
[42] R. Tholkappiyan, A.N. Naveen, K. Vishista, F. Hamed, Investigation on the electrochemical performance of hausmannite Mn3O4 nanoparticles by ultrasonic irradiation assisted co-precipitation method for supercapacitor electrodes, J. Taibah Univ. Sci. 12 (2018) 669–677.
[43] J. Chastain, R.C. King Jr, Handbook of X-ray photoelectron spectroscopy, Perkin-Elmer Corporation 40 (1992) 221.
[44] E.S. Ilton, J.E. Post, P.J. Heaney, F.T. Ling, S.N. Kerisit, XPS determination of Mn oxidation states in Mn (hydr) oxides, Appl. Surf. Sci. 366 (2016) 475–485.
[45] H. Saravaia, H. Gupta, V. Kulshrestha, Single step synthesis of a magnesium doped lithium manganese oxide ion sieve nanomaterial and a SPES/ion sieve composite membrane for the separation of lithium, RSC Adv. 6 (2016) 106980–106989.
[46] V. Pp, In vitro biocompatibility and antimicrobial activities of zinc oxide nanoparticles (ZnO NPs) prepared by chemical and green synthetic route—a comparative study, BioNanoScience 10 (2020) 112–121.
[47] A. Kołodziejczak-Radzimska, E. Markiewicz, T. Jesionowski, Structural characterisation of ZnO particles obtained by the emulsion precipitation method, J. Nanomater. 2012 (2012).
[48] L.-X. Li, D. Xu, X.-Q. Li, W.-C. Liu, Y. Jia, Excellent fluoride removal properties of porous hollow MgO microspheres, New J. Chem. 38 (2014) 5445–5452.
[49] V.K. Gupta, R. Kumar, A. Nayak, T.A. Saleh, M. Barakat, Adsorptive removal of dyes from aqueous solution onto carbon nanotubes: a review, Adv. Colloid Interface Sci. 193 (2013) 24–34.
[50] A. Bekhoukh, I. Moulefera, F.Z. Zeggai, A. Benyoucef, K. Bachari, Anionic methyl orange removal from aqueous solutions by activated carbon reinforced conducting polyaniline as adsorbent: synthesis, characterization, adsorption behavior, regeneration and kinetics study, J. Polym. Environ. (2021) 1–10.
[51] N. Kumar, G.K. Inwati, E.M. Ahmed, C. Lal, B. Makwana, V.K. Yadav, S. Islam, H. J. Ahn, K.K. Yadav, B.H. Jeon, Modified 7-Chloro-11 H-indeno [1, 2-b] quinoxaline heterocyclic system for biological activities, Catalysts 12 (2) (2022) 213.
[52] K. Rosli, A.S. Abdulhameed, S. Surip, Z.A. ALOthman, A.H. Jawad, An eco-friendly adsorbent of chitosan/montmorillonite/algae for removal of basic green 1 and reactive blue 19 dyes: Box-Behnken design optimization mechanistic study, J. Polym. Environ. (2023) 1–18.
[53] J. Wang, Y. Xia, X. Yao, M. Zhang, Y. Zhang, Z. Liu, Synthesis and electrochemical feature of a multiple-phases Li-rich nickel manganese oxides cathode material, Int. J. Electrochem. Sci. 6 (2011) 6670–6681.
[54] X. Liu, Y. Wu, H. Ye, J. Chen, W. Xiao, W. Zhou, Z.N. Garba, I. Lawan, L. Wang, Z. Yuan, Modification of sugar-based carbon using lanthanum and cobalt bimetal species for effective adsorption of methyl orange, Environ. Technol. Innov. 23 (2021) 101769.
[55] A.H. Jawad, A.S. Abdulhameed, R. Selvasembian, Z.A. ALOthman, L.D. Wilson, Magnetic biohybrid chitosan-ethylene glycol diglycidyl ether/magnesium oxide/Fe3O4 nanocomposite for textile dye removal: Box-Behnken design optimization and mechanism study, J. Polym. Res. 29 (2022) 207.
[56] Z.M. Zain, A.S. Abdulhameed, A.H. Jawad, Z.A. ALOthman, Z.M. Yaseen, A pH-sensitive surface of chitosan/sepiolite clay/algae biocomposite for the removal of malachite green and remazol brilliant blue R dyes: optimization and adsorption mechanism study, J. Polym. Environ. 31 (2023) 501–518.
[57] N. Ahmad, F.S. Arsyad, I. Royani, A. Lesbani, Adsorption of methylene blue on magnetite humic acid: kinetic, isotherm, thermodynamic, and regeneration studies, Results Chem. 4 (2022) 100629.
[58] H. Moussout, H. Ahlafi, M. Aazza, H. Maghat, Critical of linear and nonlinear equations of pseudo-first order and pseudo-second order kinetic models, Karbala Int. J. Mod. Sci. 4 (2018) 244–254.
[59] A.S. Abdulhameed, A.H. Jawad, M. Ridwan, T. Khadiran, L.D. Wilson, Z.M. Yaseen, Chitosan/carbon-doped TiO2 composite for adsorption of two anionic dyes in solution and gaseous SO2 capture: experimental modeling and optimization, J. Polym. Environ. 30 (2022) 4619–4636.
[60] B.K. Martini, T.G. Daniel, M.Z. Corazza, A.E. de Carvalho, Methyl orange and tartrazine yellow adsorption on activated carbon prepared from boiler residue: kinetics, isotherms, thermodynamics studies and material characterization, J. Environ. Chem. Eng. 6 (2018) 6669–6679.
[61] R. Lafi, A. Hafiane, Removal of methyl orange (MO) from aqueous solution using cationic surfactants modified coffee waste (MCWs), J. Taiwan Inst. Chem. Eng. 58 (2016) 424–433.
[62] B. Zhang, Y. Wu, L. Cha, Removal of methyl orange dye using activated biochar derived from pomelo peel wastes: performance, isotherm, and kinetic studies, J. Dispers. Sci. Technol. (2019).
[63] B.B. Mohammed, H. Lgaz, A.A. Alrashdi, K. Yamni, N. Tijani, Y. Dehmani, H. El Hamdani, I.-M. Chung, Insights into methyl orange adsorption behavior on a cadmium zeolitic-imidazolate framework Cd-ZIF-8: a joint experimental and theoretical study, Arab. J. Chem. 14 (2021) 102897.

[64] R.J. da Silva, L.C. Mojica-Sánchez, F.D. Gorza, G.C. Pedro, B.G. Maciel, G. P. Ratkovski, H.D. da Rocha, K.T. do Nascimento, J.C. Medina-Llamas, A. E. Chávez-Guajardo, Kinetics and thermodynamic studies of Methyl Orange removal by polyvinylidene fluoride-PEDOT mats, J. Environ. Sci. 100 (2021) 62–73.

[65] R.K. Ibrahim, A. El-Shafie, L.S. Hin, N.S.B. Mohd, M.M. Aljumaily, S. Ibraim, M. A. AlSaadi, A clean approach for functionalized carbon nanotubes by deep eutectic solvents and their performance in the adsorption of methyl orange from aqueous solution, J. Environ. Manage. 235 (2019) 521–534.

[66] T.M. Albayati, Application of nanoporous material MCM-41 in a membrane adsorption reactor (MAR) as a hybrid process for removal of methyl orange, Desalin. Water Treat. 151 (2019) 138–144.

[67] M.A. Nazir, N.A. Khan, C. Cheng, S.S.A. Shah, T. Najam, M. Arshad, A. Sharif, S. Akhtar, A. ur Rehman, Surface induced growth of ZIF-67 at Co-layered double hydroxide: removal of methylene blue and methyl orange from water, Appl. Clay Sci. 190 (2020) 105564.

[68] E.A. Mohamed, A.Q. Selim, S.A. Ahmed, L. Sellaoui, A. Bonilla-Petriciolet, A. Erto, Z. Li, Y. Li, M.K. Seliem, H2O2-activated anthracite impregnated with chitosan as a novel composite for Cr (VI) and methyl orange adsorption in single-compound and binary systems: modeling and mechanism interpretation, Chem. Eng. J. 380 (2020) 122445.

[69] J. Xu, P. Du, W. Bi, G. Yao, S. Li, H. Liu, Graphene oxide aerogels co-functionalized with polydopamine and polyethylenimine for the adsorption of anionic dyes and organic solvents, Chem. Eng. Res. Des. 154 (2020) 192–202.